Electronic Supplementary Information (ESI)

Nanostructured IrO_x supported on N-doped TiO_2 as an efficient electrocatalyst towards acidic oxygen evolution reaction

Guoqiang Li,*[a] Hongrui Jia,[a] Huan Liu,[b] Xin Yang,[a] Meng-Chang Lin[a]

[a] College of Energy Storage Technology, Shandong University of Science and Technology, Qingdao 266590, China

[b] Qingdao Institute of Bioenergy and Bioprocess Technology, Chinese Academy of Sciences, Qingdao 266101, China

* E-mail: ligq@sdust.edu.cn

1. Experimental Section

1.1 Materials

$H_2IrCl_6 \cdot xH_2O$, TiO_2 and hexadecyl trimethyl ammonium bromide (CTAB) were purchased from Aladdin Co., Ltd. Ethylene glycol (EG), isopropyl alcohol, ethanol and H_2SO_4 were purchased from Beijing Chemical Co. High-purity NH_3 gas was purchased from Ludong Gas Co. 5 wt% Nafion® solution and Nafion® 115 membrane were purchased from DuPont Co. Carbon paper was purchased from Toray Co. Commercial IrO_2 denoted as IrO_2(CM) was purchased from Alfa Aesar Chemical Co., Ltd. Commercial Pt/C (20 wt%Pt) denoted as Pt/C(CM) was purchased from Johnson Matthey Company. Commercial F-SnO_2 (FTO) conductive glass was purchased from the NSG Co., Ltd., the thickness is 1.1 mm, and the square resistance is 10 Ω. All solutions used were modulated using Millipore-MiliQ water (resistivity: ρ > 18 MΩ*cm).

1.2 Catalysts preparation

The TiO_2 powder was placed in a tubular oven and then heated to 500 °C with the heating rate of 5 °C min^{-1} and maintained for 2 h in a flowing NH_3 atmosphere. After naturally cooling to room temperature, N-doped TiO_2 (denoted as N-TiO_2) was obtained.

The IrO_x/N-TiO_2 electrocatalyst was synthesized through refluxing reduction method, in which ethylene glycol (EG) and hexadecyl trimethyl ammonium bromide (CTAB) act as the reducing and dispersing agents, respectively. At first, 50 mg N-TiO_2 and a certain amount of CTAB (nCTAB : nIr = 3:1) were ultrasonically dispersed in EG solution for 1 h. Then, 5 mL $H_2IrCl_6 \cdot xH_2O$ solution (10 mg Ir per 1 mL EG) was added, and stirred for 2 h at room temperature. Subsequently, the mixture was transferred to oil bath to react at 160 °C for 3 h. Finally, the catalyst was obtained through centrifuged with deionized water, and dried at 60 °C in the oven over night. Meanwhile, IrO_x/TiO_2 and IrO_x counterparts were synthesized through the similar procedure.

1.3 Physical characterizations

The electrical conductivity was measured using the four-point probe measurement (RTS-8, China), the sheet samples were prepared through a tablet machine (MRX-YP180, China). The crystal structure was investigated by X-ray diffraction (XRD) measurement using D8-Advance X-ray diffractometer (BRUKER Company, Germany) with the Cu Kα (l ¼1.5405 Å) as radiation source operating at 40 kV and 200 mA. The morphology feature was researched with transmission electron microscopy (TEM), high-resolution TEM (HRTEM), high-angle annular dark-field scanning TEM (HAADF-STEM), elemental mapping analysis and energy-dispersive X-ray spectroscopy (EDX) (FEI Company, USA). The surface information was proved by X-ray photoelectron spectroscopy (XPS) spectrometer (Kratos Ltd. XSAM-800, UK) with Al Kα monochromatic source. The electrochemically dissolved quantity of Ir during the stability test was determined by inductively coupled plasma optical emission spectroscopy (ICP-OES).

1.4 Electrochemical measurements

Electrochemical measurements were firstly performed with three-electrode setup operated on Princeton Applied Research Model273 Potentiostat/Galvanostat. Glassy carbon (GC, 3 mm diameter) electrode was used as the working electrode substrate, saturated calomel electrode (Hg/Hg_2Cl_2; SCE) and Pt plate were used as the reference and counter electrode, respectively. The electrolyte solution was 0.5 mol L^{-1} (0.5 M) H_2SO_4 purged with high-purity N_2. All the potentials were calibrated with the reversible hydrogen electrode (RHE) that E (RHE) = E (SCE) + 0.242 V + 0.059*pH. The working electrode was prepared as follows: 3 mg of the catalyst was firstly ultrasonically dispersed in 315 μL solutions containing of 15 μL Nafion® solution and 300 μL ethanol solution for 30 min. Then, 2.23 μL catalyst inks was pipetted and spread on the glassy carbon substrate. Finally, the working electrode was obtained after the solvent volatilized with the catalyst loading was 0.3 mg cm^{-2}.

The outer charge (Q_{outer}) was calculated from the cyclic voltammetry (CV) curves (0-1.50 V) obtained at the scanning rate of 300 mV s^{-1}, E was selected with the potential window between 0.70 and 1.40 V.

Linear sweep voltammetry (LSV) curves were recorded in the potential window

ranged from 1.10 to 1.70 V at the scanning rate of 5 mV s^{-1}. All data were corrected for 95% *iR* potential drop, and *R* is the solution resistance. The EIS measurements were applied in the frequency range of 0.1 Hz to 10 kHz at the potential of 1.55 V. The galvanostatic tests at the constant current density of 10 mA cm^{-2} for 10 h in N_2-saturated 0.5 M H_2SO_4 solution were measured by employing F-SnO_2 conductive glass (FTO, 1*2 cm) as the working electrode substrate, the catalyst loading was also 0.3 mg cm^{-2}.

Two-electrode overall water splitting tests were performed with IrO_x/N-TiO_2, IrO_x or IrO_2(CM) as the anode catalyst, and Pt/C(CM) as the cathode catalyst. FTO (1*2 cm) was used as the working electrode substrate. The anode catalyst loading was 0.3 mg cm^{-2}, and the cathode catalyst loading was 0.1 mg cm^{-2}. LSV experiments were performed with a voltage window ranged from 1.0 to 2.0 V at the scanning rate of 5 mV s^{-1} in 0.5 M H_2SO_4 at room temperature. The galvanostatic tests were performed at the constant current density of 10 mA cm^{-2} for 20 h.

1.5 Performance evaluation of the PEMWE single cell

SPEWE here can be depicted as proton exchange membrane water electrolysis (PEMWE) by using Nafion proton exchange membrane as the SPE. As the key component, membrane electrode assembly (MEA) of 12.5 cm^2 was fabricated by anode catalyst (IrO_x/N-TiO_2 or IrO_2(CM)), anode diffusion layer (Ti mesh of 4 cm diameter), cathode catalyst (Pt/C(CM)), cathode diffusion layer (carbon paper), and Nafion® 115 membrane. Specifically, the catalyst slurry was firstly prepared through mixing the catalyst powder, Nafion® solution, isopropyl alcohol and deionized water. Subsequently, the catalyst slurry was ultrasonically sprayed onto each side of membrane to form catalyst coated membrane (CCM) electrode, the anode and cathode catalyst loadings were 2.0 and 1.0 mg cm^{-2}, respectively. Finally, CCM was hot pressed with the anode-cathode diffusion layers at 120 °C and 2 MPa for 1 min. SPE water electrolysis single cell was assembled with the prepared MEA and other component such as bipolar plate, end plate, seal framework, etc. Deionized water was pumped into the anode side with the flow rate of 50 cc min^{-1}, then the single cell was connected to the Arbin battery testing instrument. The steady-state polarization tests

were performed at the water temperature of 80 °C, with the increasing current density from 0.02 to 2.0 A cm^{-2}. The stability test were performed in galvanostatic mode with the constant current densities of 0.5 and 2.0 A·cm^{-2} for 300 h, respectively.

2. Supplementary Figures and Tables

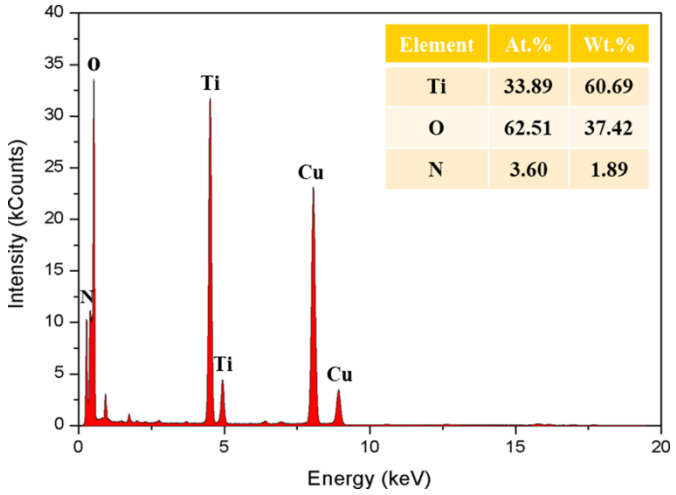

Fig. S1 EDX spectrum and element content of N-TiO_2.

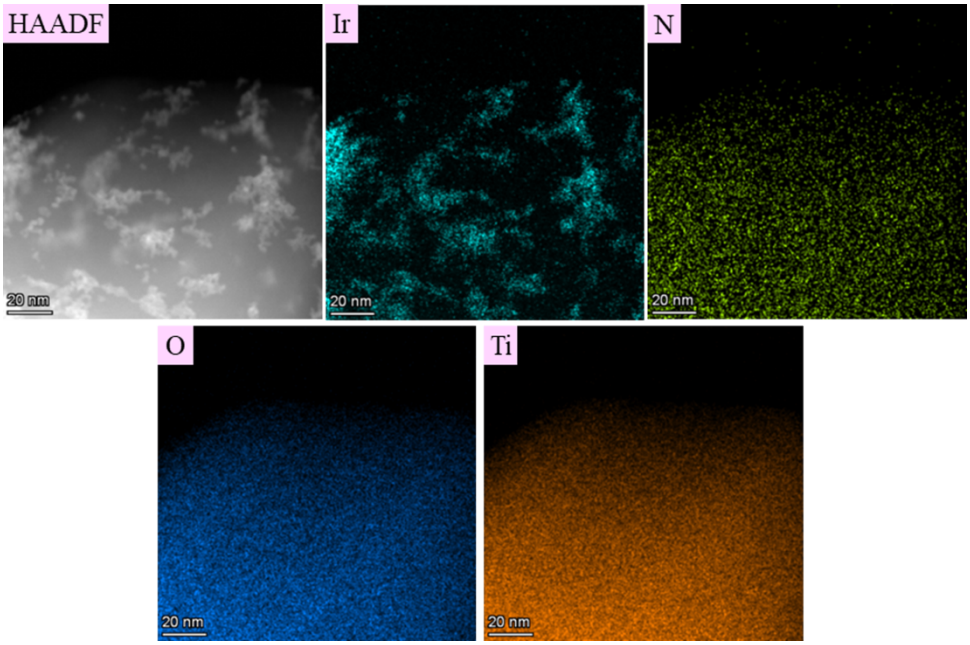

Fig. S2 HAADF-STEM and corresponding elemental mapping images of IrO_x/N-TiO_2.

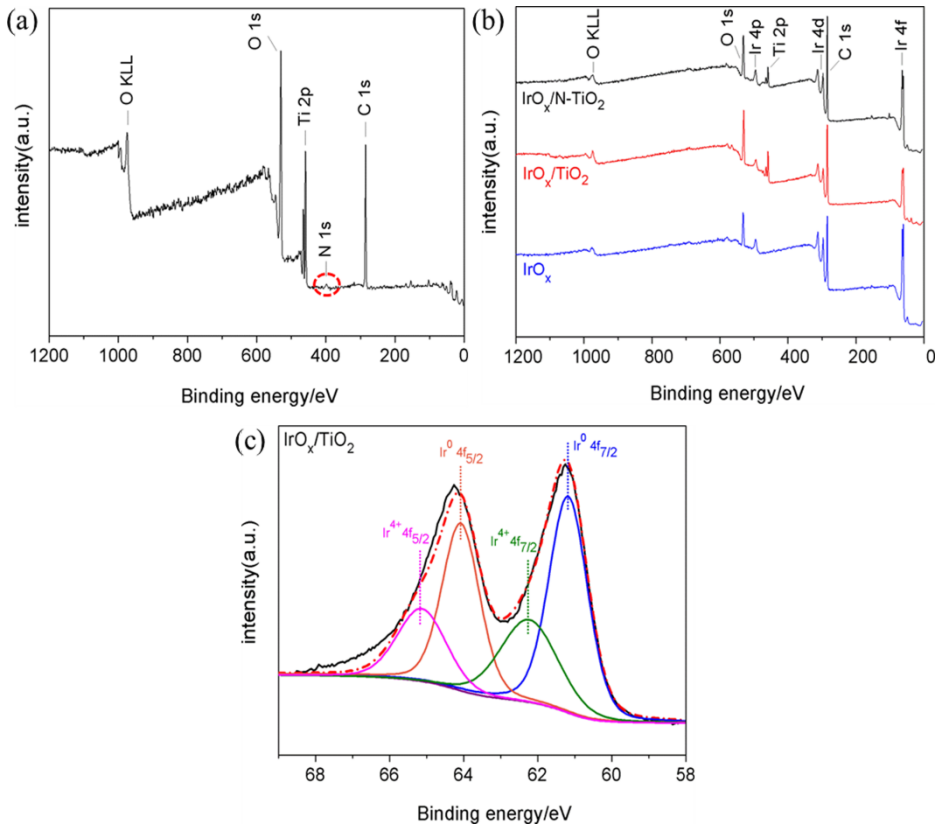

Fig. S3 (a) XPS survey spectrum for N-TiO_2. (b) XPS survey spectra for the catalysts. (c) High-resolution XPS spectra of the deconvoluted Ir 4f for IrO_x/TiO_2.

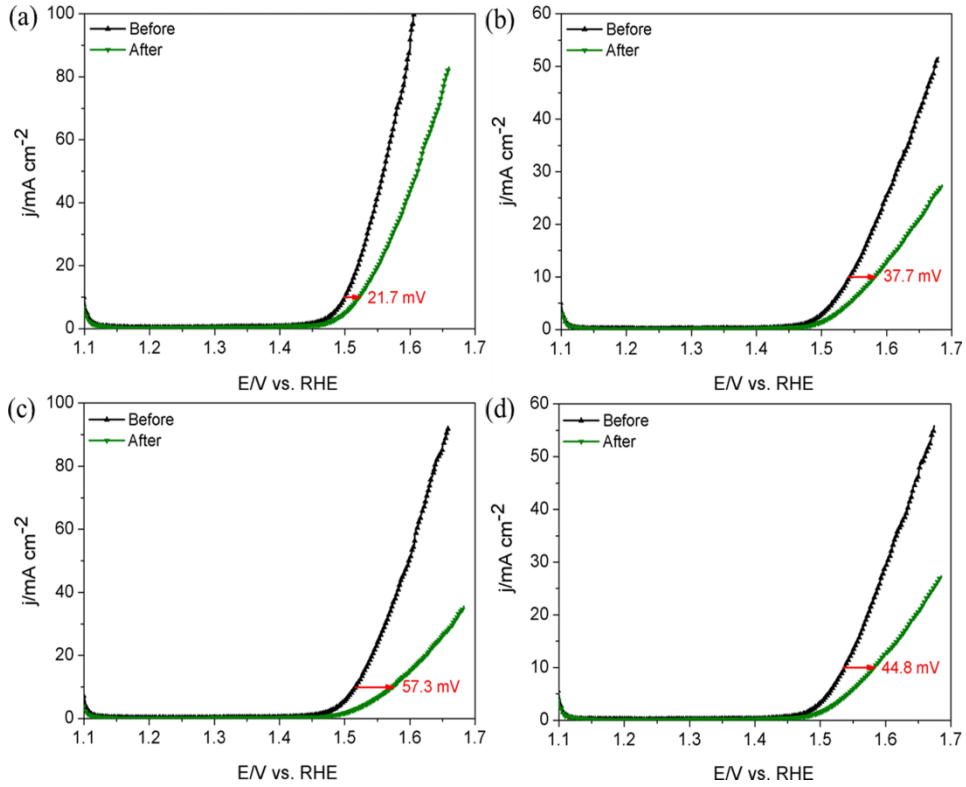

Fig. S4 LSV curves before and after the stability tests of (a) IrO_x/N-TiO_2, (b) IrO_x/TiO_2, (c) IrO_x and (d) IrO_2(CM) at the scanning rate of 5 mV s^{-1} in N_2-saturated 0.5 M H_2SO_4 at room temperature.

Table S1 XPS analysis of the catalysts.

Catalyst	Binding energy (Ir $4f_{7/2}$; eV)	Relative content (%) of Ir species	
		Ir^0	Ir^{4+}
IrO_x/N-TiO_2	61.10	66.1%	33.9%
IrO_x/TiO_2	61.26	64.1%	35.9%
IrO_x	61.34	63.2%	36.8%

Table S2 The comparison of the overpotential for IrO_x/N-TiO_2 with reported supported Ir-based electrocatalysts for acidic OER.

Catalyst	Loading (mg cm^{-2})	Electrolyte	Scanning rate (mV/s)	Current density (j, mA cm^{-2})	**Overpotential (mV vs. RHE)@j**	References
IrO_x/N-TiO_2	0.3	0.5 M H_2SO_4	5	1	195	This work
				10	270	
Ir@TiO_2	0.37	0.5 M H_2SO_4	5	10	220	1
IrO_2/TiO_2	0.2 mg_{IrO2} cm^{-2}	0.5 M H_2SO_4	1	12	370	2
Ir/Ti_4O_7	0.133	0.5 M H_2SO_4	5	10	~340	3
IrO_2/$Nb_{0.05}Ti_{0.95}O_2$	0.255	0.5 M H_2SO_4	5	1	270	4
IrO_2/Nb-TiO_2	0.23	0.1 M $HClO_4$	5	10	~310	5
IrO_2@Ir/TiN	0.379	0.5 M H_2SO_4	5	10	265	6
TiN/IrO_2	0.255	0.5 M H_2SO_4	10	10	313	7
Ir/TiC	0.122	0.1 M $HClO_4$	10	10	>320 vs. SHE	8
Ir-ND/ATO	0.0102 mg_{Ir} cm^{-2}	0.05 M H_2SO_4	5	10	>370	9
IrO_2/ATO	0.2	0.1 M $HClO_4$	5	10	256	10
IrO_2/Sb-SnO_2 NW	0.25	0.5 M H_2SO_4	1	10	8 vs. SCE	11
$Ir_{0.5}Ru_{0.5}O_2$/ATO	0.8	0.5 M H_2SO_4	0.5	1	240	12
Ir/ITO	0.102 mg_{Ir} cm^{-2}	0.1 M $HClO_4$	25	10	340	13
IrO_2/V_2O_5	0.1 mg_{Ir} cm^{-2}	0.5 M H_2SO_4	1	10	266	14

Table S3 The comparison of the mass activity for IrO_x/N-TiO_2 with reported supported Ir-based electrocatalysts for acidic OER.

Catalyst	Loading (mg cm^{-2})	Electrolyte	Scanning rate (mV/s)	Potential (V vs. RHE)	**Mass activity (A g_{Ir}^{-1})**	References
IrO_x/N-TiO_2	0.3	0.5 M H_2SO_4	5	1.48	29.4	This work
				1.50	66.1	
				1.55	278.7	
				1.60	597.7	
Ir@TiO_2	0.37	0.5 M H_2SO_4	5	1.50	486	1
Ir/Ti_4O_7	0.133	0.5 M H_2SO_4	5	1.48	4.2	3
IrO_2/$Nb_{0.05}Ti_{0.95}O_2$	0.255	0.5 M H_2SO_4	5	1.60	471 A g_{IrO2}^{-1}	4
IrO_2@Ir/TiN	0.379	0.5 M H_2SO_4	5	1.60	480.4	6
TiN/IrO_2	0.255	0.5 M H_2SO_4	10	1.60	874 A g_{IrO2}^{-1}	7
Ir/TiC	0.122	0.1 M $HClO_4$	10	1.55	150	8
Ir-ND/ATO	0.0102 mg_{Ir} cm^{-2}	0.05 M H_2SO_4	5	1.51	70	9
				1.60	135.8	
IrO_2/ATO	0.2	0.1 M $HClO_4$	5	1.60	120	10
Ir/ITO	0.102 mg_{Ir} cm^{-2}	0.1 M $HClO_4$	25	1.48	16	13
IrO_2/V_2O_5	0.1 mg_{Ir} cm^{-2}	0.5 M H_2SO_4	1	1.53	287	14
Ir/ATO	0.203	0.5 M H_2SO_4	0.167	1.48 vs. Ag/AgCl	845	15
IrO_2/ATO	--	0.5 M H_2SO_4	10	1.53	63	16
IrO_2/ meso-Sb-SnO_2	0.102	0.5 M H_2SO_4	5	1.60	459.1	17

Table S4 R_s and R_{ct} component values analyzed from the EIS tests.

Catalyst	R_s (Ω)	R_{ct} (Ω)
IrO_x/N-TiO_2	5.5	14.5
IrO_x/TiO_2	5.8	35.3
IrO_x	5.7	20.6
IrO_2(CM)	5.7	33.4

References

(1) J. Y. Chen, S. Jayabal, D. S. Geng and X. Hu, *ChemistrySelect*, 2021, **6**, 9134-9138.

(2) Z. X. Lu, Y. Shi, C. F. Yan and C. Q. Guo, *Int. J. Hydrogen Energy*, 2017, **42**, 3572-3578.

(3) L. Wang, P. Lettenmeier, U. Golla-Schindler, P. Gazdzicki, N. A. Cañas, T. Morawietz, R. Hiesgen, S. S. Hosseiny, A. S. Gago and K. A. Friedrich, *Phys. Chem. Chem. Phys.*, 2016, **18**, 4487-4495.

(4) W. Hu, S. L. Chen and Q. H. Xia, *Int. J. Hydrogen Energy*, 2014, **39**, 6967-6976.

(5) C. P. Hao, H. Lv, C. E. Mi, Y. K. Song and J. X. Ma, *ACS Sustainable Chem. Eng.*, 2016, **4**, 746-756.

(6) G. Q. Li, K. Li, L. Yang, J. F. Chang, R. P. Ma, Z. J. Wu, J. J. Ge, C. P. Liu and W. Xing, *ACS Appl. Mater. Interfaces*, 2018, **10**, 38117-38124.

(7) K. K. Zhang, W. S. Mai, J. Li, H. Wang, G. Q. Li and W. Hu, *J. Mater. Sci.*, 2020, **55**, 3507-3520.

(8) R. E. Fuentes, H. R. Colón-Mercado and M. J. Martínez-Rodríguez, *J. Electrochem. Soc.*, 2013, **161**, F77-F82.

(9) H-S. Oh, H. N. Nong, T. Reier, M. Gliech and P. Strasser, *Chem. Sci.*, 2015, **6**, 3321-3328.

(10) S-B. Han, Y-H. Mo, Y-S. Lee, S-G. Lee, D-H. Park and K-W. Park, *Int. J. Hydrogen Energy*, 2020, **45**, 1409-1416.

(11) G. Liu, J. Xu, Y. Wang and X. Wang, *J. Mater. Chem. A*, 2015, **3**, 20791-20800.

(12) A. T. Marshall and R. G. Haverkamp, *Electrochim. Acta*, 2010, **55**, 1978-1984.

(13) D. Lebedev and C. Copéret, *ACS Appl. Energy Mater.*, 2019, **2**, 196-200.
(14) X. Zheng, M. Qin, S. Ma, Y. Chen, H. Ning, R. Yang, S. Mao and Y. Wang, *Adv. Sci.*, 2022, **9**, 2104636.
(15) F. Karimi and B. A. Peppley, *Electrochim. Acta*, 2017, **246**, 654-670.
(16) D. Böhm, M. Beetz, M. Schuster, K. Peters, A. G. Hufnagel, M. Döblinger, B. Böller, T. Bein and D. Fattakhova-Rohlfing, *Adv. Funct. Mater.*, 2019, **30**, 1906670.
(17) J. Tong, Y. Liu, Q. Peng, W. Hu and Q. Wu, *J. Mater. Sci.*, 2017, **52**, 13427-13443.